Single quantum dot nanowire photodetectors

M. P. van Kouwen,[1] M. H. M. van Weert,[1] M. E. Reimer,[1] N. Akopian,[1] U. Perinetti,[1]
R. E. Algra,[2,a)] E. P. A. M. Bakkers,[1,b)] L. P. Kouwenhoven,[1] and V. Zwiller[1,c)]

[1]*Kavli Institute of Nanoscience, Delft University of Technology, Delft, Zuid Holland 2628CJ, The Netherlands*
[2]*Philips Research Eindhoven, Eindhoven, Noord Brabant 5600AE, The Netherlands*

We report InP nanowire photodetectors with a single InAsP quantum dot as light absorbing element. With excitation above the InP band gap, the nanowire photodetectors are efficient (quantum efficiency of 4%). Under resonant excitation of the quantum dot, the photocurrent amplitude depends on the linear polarization direction of the incident light. The photocurrent is enhanced (suppressed) for a polarization parallel (perpendicular) to the axis of the nanowire (contrast 0.83). The active detection volume under resonant excitation is 7×10^3 nm^3. These results show the promising features of quantum dots embedded in nanowire devices for electrical light detection at high spatial resolution. © *2010 American Institute of Physics.* [doi:10.1063/1.3484962]

Nanowires (NWs) offer a large material design freedom since materials of different lattice constants can be combined. The large surface to volume ratio of the NWs is beneficial for detection of viruses[1] and gases.[2] In addition, NW devices have shown excellent light detection properties.[3–6] Recently, quantum dots (QDs) embedded in NW devices have shown both single electron control[7–10] and single photon emission,[11] which are important in quantum information applications. The unique combination of an on-chip light emitter and detector is useful for near field optical circuits using plasmon waveguides.[12] Although electrically driven light emission from NWs and NW-QDs have been reported,[13–15] electrical light detection using NW-QDs has not been studied extensively. Here we present InP NW photodetectors containing a single InAsP QD. InP is a suitable material for efficient electrical photon detection since it has a high absorption coefficient (3.1×10^4 cm^{-1} at 1.5 eV photon energy);[16] a high electron mobility (10^3 cm^2/V s), a long minority carrier diffusion length ($1–2$ μm) and a low surface recombination velocity (10^3 cm/s).[17]

The InP NWs studied here are unintentionally doped and have typical lengths of 4 μm and tapered diameters ranging from 20 to 60 nm.[10] The NWs were grown by metal-organic vapor phase epitaxy, using 20 nm gold colloids as catalysts for vapor liquid solid nucleation.[18] The InAs$_{0.25}$P$_{0.75}$ QD is (5 ± 2) nm high with (33 ± 1) nm diameter and is positioned in the middle of the NW.[19] The contacts consist of a titanium (110 nm)/aluminum (10 nm) thin film. The processing of these NW-QD devices has been described in detail elsewhere.[10]

In Fig. 1, we present the photoresponse and carrier dynamics of a single NW photodetector at low temperature (T=10 K). The device geometry and circuit schematics (inset) are shown in Fig. 1(a). The applied voltage difference between the two contacts to the NW (source and drain) is depicted by V_{sd}. In Fig. 1(b), the photocurrent of the NW as a function of V_{sd} is presented. The photodetector is excited

with photons of 1.5 eV, close to the band gap of the wurtzite InP NW, at laser intensities of 430 W/cm^2 (top trace) and 20 W/cm^2 (middle trace). In the bias range of $0 < V_{sd} < 1$ V, an exponential photocurrent increase is observed in the current-voltage characteristic (I-V) due to the Schottky nature of the two contacts. Above V_{sd}=2 V, the photocurrent increases linearly with applied bias. At V_{sd}=6 V and under an excitation intensity of 430 W/cm^2, the detector generates a photoexcited current of ~400 pA. The dark current (bottom trace) is lower than 0.5 pA up to V_{sd}=6 V. The two
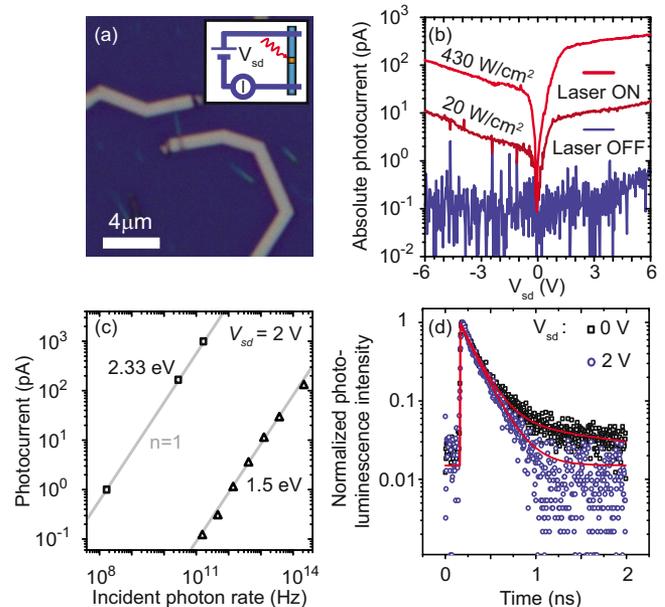
FIG. 1. (Color online) The NW photodetector. (a) Device geometry and working principle. Optical micrograph image shows a contacted NW forming the QD photodetector. Inset: circuit schematics. (b) Illuminated (430 W/cm^2, top line; 20 W/cm^2, middle line; 1.5 eV) and dark noise (bottom line) current-voltage characteristic of the photodetector. (c) Incident photon rate dependence of the photocurrent for excitation with an energy of 2.33 eV (squares) and 1.5 eV (triangles). Gray lines indicate linear intensity dependence (n=1) (T=10 K, V_{sd}=2 V). (d) Time resolved PL measurement under pulsed optical excitation for V_{sd}=0 V (squares) and 2 V (circles). Data obtained using a streak-camera. Lines represent exponential fits to the decay (excitation intensity=100 kW/cm^2 focused to a spot size of ≤ 1 μm, photon energy=1.5 eV, T=10 K, collection energy range of 1.37–1.49 eV, integration time 600 s).

a)Also at Materials Innovation institute (M2I), Delft, The Netherlands and IMM, Solid State Chemistry, Radboud University, Nijmegen, The Netherlands.
b)Also at Eindhoven University of Technology, The Netherlands.
c)Electronic mail: v.zwiller@tudelft.nl.

97, 113108-1

Schottky contacts and the low carrier concentration in the NW produce a high signal to noise ratio ($\sim$800) in the photodetection and allow for the application of an electric field along the NW axis.[10] Since the laser is aligned to the QD, the asymmetry in the I-V indicates that the QD is positioned closer to the drain contact.[20]

In Fig. 1(c) we present the photocurrent as a function of incident photon rate ϕ (calculated from the NW diameter, the laser spot size and power, under the assumption of total absorption) at a source-drain bias of $V_{sd}=2$ V for two excitation energies: at the InP band edge (1.5 eV, triangles) and well above the band gap (2.33 eV, squares). The photocurrent increases linearly with excitation intensity for both excitation energies. Here, we obtain a linear dependence over three orders of magnitude, comparable to core shell p-i-n NW diodes.[6] From the linear dependence, the total quantum efficiency (QE=$I/e\phi$) at $V_{sd}=2$ V is determined to be $(2.13\pm0.04)\times10^{-6}$ (1.5 eV excitation) and $(4.1\pm0.1)\times10^{-2}$ (2.33 eV excitation), indicating that the absorption highly depends on the excitation photon energy. The corresponding noise equivalent power (NEP) of the detector is 10^{-9} W/$\sqrt{\text{Hz}}$ (1.5 eV) and 10^{-13} W/$\sqrt{\text{Hz}}$ (2.33 eV), where NEP is defined as $(h\nu/\text{QE})*(D/e)$, where D is the dark current noise (rms of 0.02 pA at $V_{sd}=2$ V, sampling frequency: 100 Hz).

We now investigate the effective lifetime of the photoexcited carriers in the NW (τ_{eff}), which depends on the applied source-drain bias. Lifetime measurements are performed under optical excitation by a laser beam focused at the QD position for two applied source-drain biases in Fig. 1(d). Here, the normalized photoluminescence (PL) intensity from the NW (the detection energy range of 1.37–1.49 eV excludes the QD photoemission) is presented as a function of time after excitation by a 2 ps laser pulse of 100 kW/cm² (laser energy=1.5 eV, laser spot size ≤1 μm). At $V_{sd}=0$ V (black squares), a biexponential decay can be fitted (upper red trace) with 180 ps and 1.5 ns time constants. The long process we attribute to recombination of trapped photoexcited carriers. One possible explanation is that the carrier trapping is caused by surface roughness/states of the NW. At $V_{sd}=2$ V (blue circles) we are able to fit a single exponential decay (lower red trace) with a time constant (τ_{eff}) of 175 ps indicating that the surface state-trapping is removed. The short lifetime indicates that stacking faults are present in the wurtzite InP NW, which has been observed before for InP NWs grown from 20 nm colloids at 420 °C and a V/III ratio of 350.[21]

In the following, the photodetection properties of the single InAsP QD embedded in the NW are presented. PL spectra of a contacted NW-QD ($V_{sd}=0$ V, laser aligned to QD position, spot size ≤1 μm) are shown in Fig. 2(a). The emission shows typical state filling of the single QD s, p, and d shells under increasing excitation intensity. More extensive optical properties are presented in earlier work.[10,19] The broad peak at 1.46 eV is attributed to wurtzite InP NW emission in the presence of zinc blende sections of varying sizes.[21] In Fig. 2(b), the integrated QD s-shell PL intensity is compared to the generated photocurrent as a function of V_{sd}. The integrated PL range is indicated by the solid-line box in Fig. 2(a). At $V_{sd}=0$ V and 10 W/cm² excitation intensity, only PL from the NW-QD is observed. Beyond $V_{sd}=1$ V, the PL intensity decreases, while the photocurrent increases,
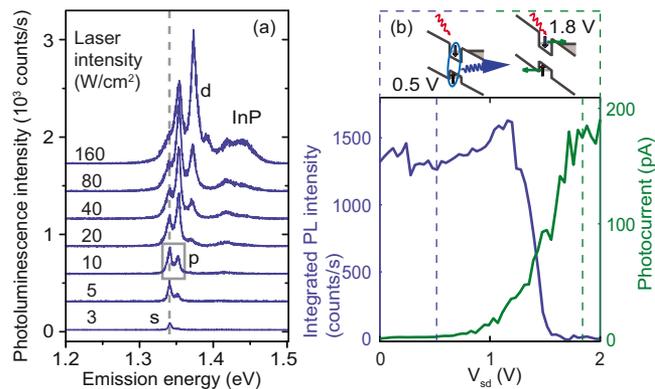
FIG. 2. (Color online) Nonresonantly excited PL and photocurrent (laser spot focused to QD position). (a) PL spectra of the QD as a function of laser excitation intensity. The box indicates PL conditions for (b) whereas the dashed line indicates QD s-shell resonance (excitation energy=2.33 eV, bias=0 V, $T=10$ K). (b) Comparison of the integrated PL intensity to the photocurrent as a function of applied source-drain bias (excitation intensity=10 W/cm², photon energy=2.33 eV, $T=10$ K, integration time =10 s). Top, band-structures of the NW photodetector QD indicating radiative recombination and tunneling processes.

thereby revealing the competing processes of photoemission and photocurrent. At $V_{sd}=2$ V, no PL is observed and the photocurrent saturates (180 pA). The two processes are presented schematically in the upper panel of Fig. 2(b). To demonstrate that the photocurrent can also be generated from the QD, the QD is resonantly excited in the following.

The spatial and polarization selectivity of the NW photodetector under resonant excitation of the QD is presented in Fig. 3. The excitation energy for these experiments is indicated in Fig. 2(a) by the dashed line. The QD volume is 7×10^3 nm³, which is two orders of magnitude smaller than the smallest previously reported active region in a NW photodetector.[22] Figure 3(a) shows the resonant photocurrent as a function of laser position on the sample. The small size of the detector enables imaging of a laser spot with the single QD photocurrent. A spot size of 0.62 ± 0.1 μm (full width at half maximum) is obtained, which corresponds to the diffraction limit of the excitation beam (NA=0.75, $\lambda=933$ nm).
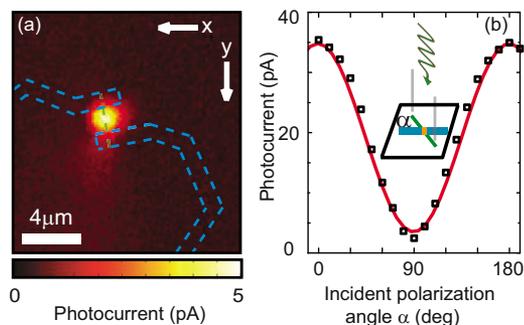
FIG. 3. (Color online) The QD photodetector. (a) Contour plot of the photocurrent as a function of laser position under resonant excitation of the QD s-shell [see Fig. 2(a), dashed line, for resonance energy]. Contacts and nanowire (dashed lines) correspond to geometry presented in Fig. 1(a) (laser intensity=30 kW/cm², incident photon energy=1.328 eV, $V_{sd}=2$ V, T =10 K). (b) Polarization dependence of the photocurrent under resonant excitation of the QD (laser intensity=200 kW/cm², photon energy =1.328 eV, $T=10$ K, $V_{sd}=6$ V). Each square represents the average current over 100×10 ms=1 s. The data fits to $\sim\cos^2(\alpha)$, which is represented by the solid line. At $\alpha=0$ the incident light is polarized along the NW axis.

In contrast to theoretical predictions,[23] it has been experimentally demonstrated that NW-QD optical excitation is most efficient under excitation of linearly polarized light in the direction parallel to the NW axis.[24] In that work, the QD was excited nonresonantly. Here, we use the photocurrent technique to resonantly excite the optically allowed *s*-shell transition and study the polarization dependence when the laser is aligned and focused to the QD [see Fig. 3(b)]. The resonant photocurrent experiment confirms the previously reported polarization anisotropy, with an enhanced photoresponse for a linear polarization parallel to the NW axis. The degree of linear polarization ρ can be obtained from the photocurrent amplitude: $\rho = I_{max} - I_{min}/I_{max} + I_{min} = 0.83$. The polarization anisotropy in the resonant excitation of the QD indicates that the absorption is influenced by the NW, which acts as an elongated and highly refracting structure. The QD ρ value of 0.83 is consistent with Mie calculations for NWs.[24] The degree of linear polarization is similar to previously reported values for nanotubes[25] and wires.[3] The total QE of the resonant QD photocurrent ranges from 3×10^{-5} (perpendicular polarization) to 2×10^{-4} (parallel polarization). We note that by assuming total absorption for the QD cross section, we underestimate the QE. On-chip waveguides could highly improve the collection efficiency of the QD.

To summarize, we presented single QDs embedded in NW photodetectors. We demonstrated a NW photocurrent QE of up to 4% with a NEP of 10^{-13} W/$\sqrt{\text{Hz}}$. In addition, we have shown that the QD photocurrent has high spatial and linear polarization selectivity. These results represent the promising features of QDs embedded in NW devices for electrical light detection at subwavelength spatial resolution. In order to obtain single photon detection, it is desirable to induce multiplication via a p-i-n junction[26] in future NW-QD photodetectors.

[1] Y. Cui, Q. Wei, H. Park, and C. M. Lieber, Science **293**, 1289 (2001).

[2] Q. Wan, Q. H. Li, Y. J. Chen, T. H. Wang, X. L. He, J. P. Li, and C. L. Lin, Appl. Phys. Lett. **84**, 3654 (2004).

[3] J. Wang, M. S. Gudiksen, X. Duan, Y. Cui, and C. M. Lieber, Science **293**, 1455 (2001).

[4] H. Pettersson, J. Trägårdh, A. I. Persson, L. Landin, D. Hessman, and L. Samuelson, Nano Lett. **6**, 229 (2006).

[5] C. Yang, C. J. Barrelet, F. Capasso, and C. M. Lieber, Nano Lett. **6**, 2929 (2006).

[6] C. Colombo, M. Heiss, M. Gratzel, and A. Fontcuberta i Morral, Appl. Phys. Lett. **94**, 173108 (2009).

[7] S. De Franceschi, J. A. van Dam, E. P. A. M. Bakkers, L. F. Feiner, L. Gurevich, and L. P. Kouwenhoven, Appl. Phys. Lett. **83**, 344 (2003).

[8] A. Pfund, I. Shorubalko, R. Leturcq, and K. Ensslin, Appl. Phys. Lett. **89**, 252106 (2006).

[9] A. Fuhrer, L. Fröberg, J. Pedersen, M. Larsson, A. Wacker, M. Pistol, and L. Samuelson, Nano Lett. **7**, 243 (2007).

[10] M. P. van Kouwen, M. E. Reimer, A. W. Hidma, M. H. M. van Weert, R. E. Algra, E. P. A. M. Bakkers, L. P. Kouwenhoven, and V. Zwiller, Nano Lett. **10**, 1817 (2010).

[11] M. T. Borgström, V. Zwiller, E. Muller, and A. Imamoglu, Nano Lett. **5**, 1439 (2005).

[12] R. W. Heeres, S. N. Dorenbos, B. Koene, G. S. Solomon, L. P. Kouwenhoven, and V. Zwiller, Nano Lett. **10**, 661 (2010).

[13] K. Haraguchi, T. Katsuyama, K. Hiruma, and K. Ogawa, Appl. Phys. Lett. **60**, 745 (1992).

[14] M. Gudiksen, L. Lauhon, J. Wang, D. Smith, and C. Lieber, Nature (London) **415**, 617 (2002).

[15] E. D. Minot, F. Kelkensberg, M. van Kouwen, J. A. van Dam, L. P. Kouwenhoven, V. Zwiller, M. T. Borgstrom, O. Wunnicke, M. A. Verheijen, and E. P. A. M. Bakkers, Nano Lett. **7**, 367 (2007).

[16] D. E. Aspnes and A. A. Studna, Phys. Rev. B **27**, 985 (1983).

[17] T. P. Pearsall, *Properties, Processing and Applications of Indium Phosphide* (Institution of Engineering and Technology, London, 2000).

[18] R. S. Wagner and W. C. Ellis, Appl. Phys. Lett. **4**, 89 (1964).

[19] M. H. M. van Weert, N. Akopian, U. Perinetti, M. P. van Kouwen, R. E. Algra, M. A. Verheijen, E. P. Bakkers, L. P. Kouwenhoven, and V. Zwiller, Nano Lett. **9**, 1989 (2009).

[20] Y. Gu, E. S. Kwak, J. L. Lensch, J. E. Allen, T. W. Odom, and L. J. Lauhon, Appl. Phys. Lett. **87**, 043111 (2005).

[21] L. M. Smith, H. E. Jackson, J. M. Yarrison-Rice, and C. Jagadish, Semicond. Sci. Technol. **25**, 024010 (2010).

[22] L. Tang, S. Kocabas, S. Latif, A. Okyay, D. Ly-Gagnon, K. Saraswat, and D. Miller, Nat. Photonics **2**, 226 (2008).

[23] Y. M. Niquet and D. C. Mojica, Phys. Rev. B **77**, 115316 (2008).

[24] M. H. M. van Weert, N. Akopian, F. Kelkensberg, U. Perinetti, M. P. van Kouwen, J. Gómez Rivas, M. T. Borgström, R. E. Algra, M. A. Verheijen, E. P. A. M. Bakkers, L. P. Kouwenhoven, and V. Zwiller, Small **5**, 2134 (2009).

[25] M. Freitag, Y. Martin, J. Misewich, R. Martel, and P. Avouris, Nano Lett. **3**, 1067 (2003).

[26] O. Hayden, R. Agarwal, and C. M. Lieber, Nature Mater. **5**, 352 (2006).